



OPEN **SHLP2 restores pre-osteoblastic cells against oxidative stress-induced inflamming**

Jeong-Hyun Ryu^{1,2,7}, Utkarsh Mangal^{3,7}, Jae-Hyung Kim¹, Dong Joo Yang⁴, Kee-Joon Lee¹, Yun-Hee Choi⁴, Dong Min Shin^{4,5}, Sung-Hwan Choi^{1,5,6} & Ki Woo Kim^{4,5}

This study aimed to evaluate the cytoprotective effects of the mitochondrial-derived peptide, Small Humanin-Like Peptide-2 (SHLP2), on pre-osteoblastic cells exposed to sub-toxic oxidative stress, with the aim of preserving bone homeostasis under conditions of inflamming. Pre-osteoblastic MC3T3-E1 cells were cultured under sub-toxic oxidative stress induced by 600 μ M H₂O₂. The study evaluated the effects of SHLP2 (at 10 μ M concentration) through assays for mitochondrial activity, reactive oxygen species (ROS) generation, apoptosis markers, and osteogenic differentiation. Quantitative polymerase chain reaction, alkaline phosphatase (ALP) staining, and Alizarin Red S biomimetic mineralization assays were performed to assess gene expression, osteogenic activity, and biomimetic mineralization. Oxidatively stressed but untreated cells served as the positive control (PC), while oxidative stress-free cells were used as the mock control. Statistical analyses were performed using one-way ANOVA and t-tests. SHLP2 treatment significantly ($p < 0.001$) improved cell viability and reduced ROS activity in oxidatively stressed cells. A significant ($p < 0.001$) decrease in apoptotic markers, including p53 and BAX, and an increase in anti-apoptotic BCL-2 levels, were observed. Additionally, SHLP2 treatment upregulated key osteogenic markers, including RUNX2, OSX, and ALP, compared to PC. When compared to the mock group, SHLP2 restored ALP activity to 95.6% by day 14. By day 21, the biomimetic mineralization assay demonstrated 94.92% activity following SHLP2 treatment. SHLP2 treatment effectively mitigates oxidative stress in pre-osteoblastic cells, providing apoptosis protection and preserving osteogenic activity. These findings underscore the potential of SHLP2 as an adjuvant therapeutic agent for enhancing the tissue microenvironment in conditions such as periodontitis and inflamming.

Keywords Small humanin-like peptide-2, Oxidative stress, Inflamming, Pre-osteoblastic cells, Periodontitis, Mitokine

The alveolar bone is a specialized connective tissue in the maxillofacial skeleton forming the periodontal structure that supports the teeth. The dynamic structure is subjected to continuous mechanical stress and undergoes constant remodeling, maintaining bone integrity and functionality. Periodontitis, a multifactorial chronic inflammatory disease, disrupts this balance¹. While controlling the microbial causes of periodontitis helps to restore bone remodeling balance, the strong association between periodontitis and systemic factors presents a significant challenge. Particularly, in aged cohorts with periodontitis, alterations in the resident cell population have been linked to increased disease severity².

Among the diverse aging phenotypes, the tissue microenvironment has emerged as a critical factor influencing disease progression². Notably, an imbalance between immune and nonimmune cell populations contributes to a steady state of elevated pro-inflammatory cytokine levels³. This phenomenon is well-known as inflamming and is characterized by chronic low-grade systemic inflammation that exacerbates oxidative stress². The persistent inflammatory state creates a negative feedback loop that impairs bone homeostasis, possibly even after

¹Department of Orthodontics, Institute of Craniofacial Deformity, Yonsei University College of Dentistry, Seoul 03722, Republic of Korea. ²Department of Biomedical Engineering, Daelim University, Anyang 13916, Republic of Korea. ³Department of Oral Biology, Yonsei University College of Dentistry, Seoul 03722, Republic of Korea.

⁴Division of Physiology, Department of Oral Biology, Yonsei University College of Dentistry, Seoul 03722, Republic of Korea. ⁵BK21 FOUR, Department of Applied Life Science, Yonsei University College of Dentistry, Seoul 03722, Republic of Korea. ⁶Center for Systems Biology, Massachusetts General Hospital, Boston, MA 02114, USA. ⁷Jeong-Hyun Ryu and Utkarsh Mangal contributed equally to this work. email: selfexam@yuhs.ac; kiwoo-kim@yuhs.ac

the microbial etiology of periodontitis has been addressed⁴. Consequently, additional therapeutic strategies that factor minimization of dysregulation at the formative cellular level are required to address local tissue damage⁵.

Chronic inflammation and oxidative stress, as observed in periodontitis, can trigger senescence⁶. Given the high prevalence of excessive reactive oxygen species (ROS) in the pathogenesis of periodontal disease and senescence-related comorbidities, mitigating oxidative stress may restore the tissue microenvironment^{7,8}. In the context of alveolar bone turnover, under oxidative stress the competitive metabolic demands for aerobic glycolysis between immune cells and osteoblasts can further undermine osteogenic capacity⁹. Therefore, addressing these underlying mechanisms is important in restoring tissue homeostasis.

Mitochondrial-derived peptides (MDPs) are a family of small bioactive polypeptides encoded by distinct open reading frames within the mitochondrial genome. Humanin (HN), the first MDP to be discovered and the best characterized to date, has been shown to counteract mitochondrial dysfunction and promote cell survival, establishing it as a prototype mitokine involved in stress adaptation and age-related disease models. Building on these insights, recent research has highlighted the crucial role of mitokines, particularly the small humanin-like peptides (SHLPs), in regulating inflammatory response and cellular metabolism¹⁰. Among these peptides, SHLP2 has been shown to enhance cell viability, reduce apoptosis, and regulate processes such as metabolism, inflammation, and programmed cell death¹¹. Beyond its antioxidant and anti-apoptotic activities, SHLP2 exhibited broad therapeutic potential in age-related or degenerative conditions, where persistent oxidative stress and impaired mitochondrial signaling contribute to tissue dysfunction¹¹. It has been shown to enhance mitochondrial respiration and antioxidant defense through activation of AMPK and P13K/Akt signaling pathways – key regulators of osteoblast differentiation, energy metabolism, and survival¹². By reinforcing mitochondrial resilience, SHLP2 may mitigate the harmful effects of ROS accumulation and inflamming, thereby contributing to a supportive tissue healing microenvironment.

Despite advances in understanding the role of inflammation in periodontitis, there is a notable lack of research on the role of mitokines. This gap is especially important considering their potential to influence the healing microenvironment and the critical role of aerobic glycolysis in bone remodeling¹³. Moreover, the beneficial effects of SHLP2 on cellular metabolism in osteoblastic cells have been sparsely investigated. To address this gap, the present study evaluates the effects of SHLP2 on pre-osteoblasts under oxidative stress induced by H₂O₂ treatment. Specifically, we investigate whether SHLP2 can promote pre-osteoblast proliferation, differentiation, and activity in an oxidatively stressed environment through apoptosis regulation (Fig. 1).

Results

Effect of SHLP2 treatment on viability and ROS activity in oxidatively stressed cells

The sub-toxic oxidative stress threshold for pre-osteoblast cells was determined using a cell viability assay with increasing H₂O₂ concentrations. A dose of 600 μ M H₂O₂, resulting in 71% cell viability, was selected (Fig. S1A). Screening with 5 μ M, 10 μ M, and 20 μ M SHLP2 showed improved viability up to 10 μ M, while 20 μ M exhibited effects similar to untreated controls (Fig. S1B). These findings established 600 μ M H₂O₂ as the sub-toxic oxidative stress condition for subsequent experiments.

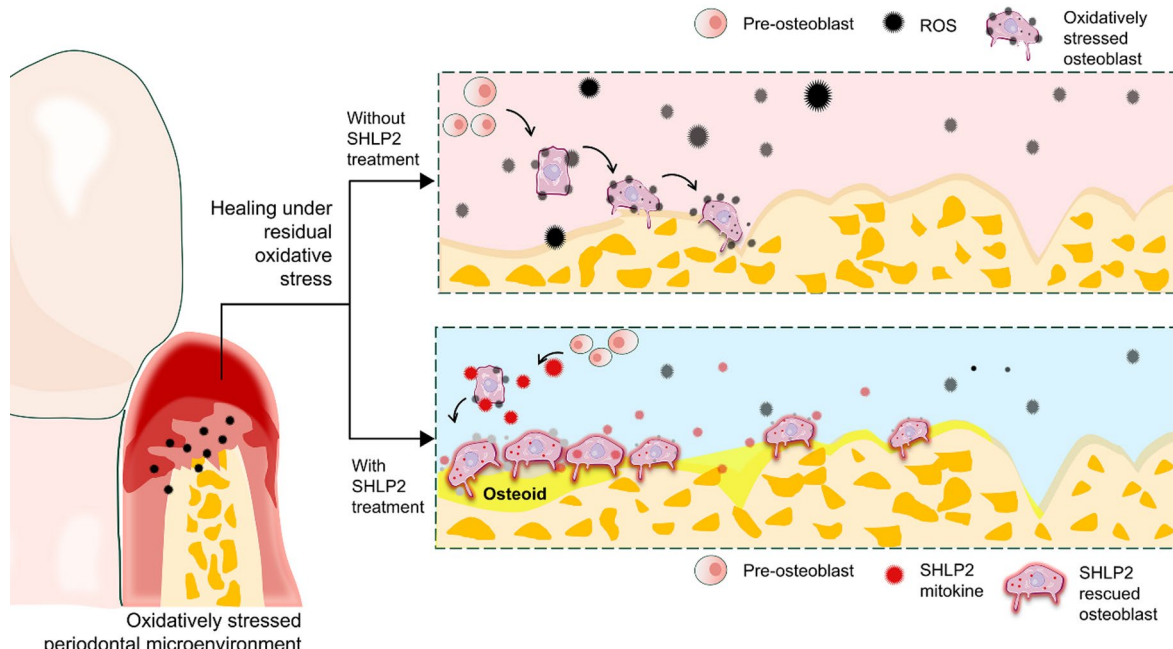


Fig. 1. Schematic illustration of small humanin-like peptide 2 (SHLP2) for recovering the impaired bone homeostasis with downregulation of the apoptotic pathway induced by reactive oxygen species (ROS) and promoting osteoblastic functional recovery.

Assessment of cellular metabolic activity indicated no significant effect of SHLP2 treatment after 24 h (Fig. 2A). However, after 3 days, treatment with 10 μ M SHLP2 resulted in an 11.6% increase in metabolic activity compared to the PC group ($p < 0.001$; Fig. 2B). Immunofluorescence analysis revealed a significant reduction in ROS levels ($p < 0.001$) following treatment with 10 μ M SHLP2 (Fig. 2C–D). In summary, 10 μ M SHLP2 demonstrated notable cellular proliferative activity and effectively inhibited ROS generation. Consequently, 10 μ M SHLP2 was selected for comparison with the PC group in subsequent analyses of anti-apoptotic and osteogenic activities.

SHLP2 modulation effect on oxidative stress and apoptotic pathway

To investigate ROS-induced apoptosis inhibition, mRNA expression levels of oxidative stress response and apoptotic signaling genes were analyzed (Fig. 3A). On day 1, SHLP2 treatment significantly increased early response marker SOD1 expression ($p < 0.001$), while SOD2 levels also showed an increase. Markers of the apoptotic cascade exhibited marked reductions, including a significant decrease in p53 expression ($p < 0.01$). Although anti-apoptotic BCL-2 levels increased with SHLP2 treatment, the change was not statistically significant (Fig. 3B). By day 3, SHLP2-treated cultures demonstrated significantly lower fold changes in both oxidative stress and apoptotic markers, suggesting enhanced resistance to sub-lethal oxidative stress (Fig. 3B, Table S2).

Enhancement of osteogenic activity with SHLP2 treatment

The functional recovery of pre-osteoblast cells was evaluated by comparing the expression of osteogenic markers in 3-day and 7-day cultures. After 3 days of treatment, significant enhancement of key osteogenic markers, OSX, and RUNX2 was observed with the highest upregulation. A marked and significant increase was also observed in BSP, ALP, SPARC, and OCN (Fig. 4A). In 7-day cultures, SHLP2 treatment consistently resulted in statistically

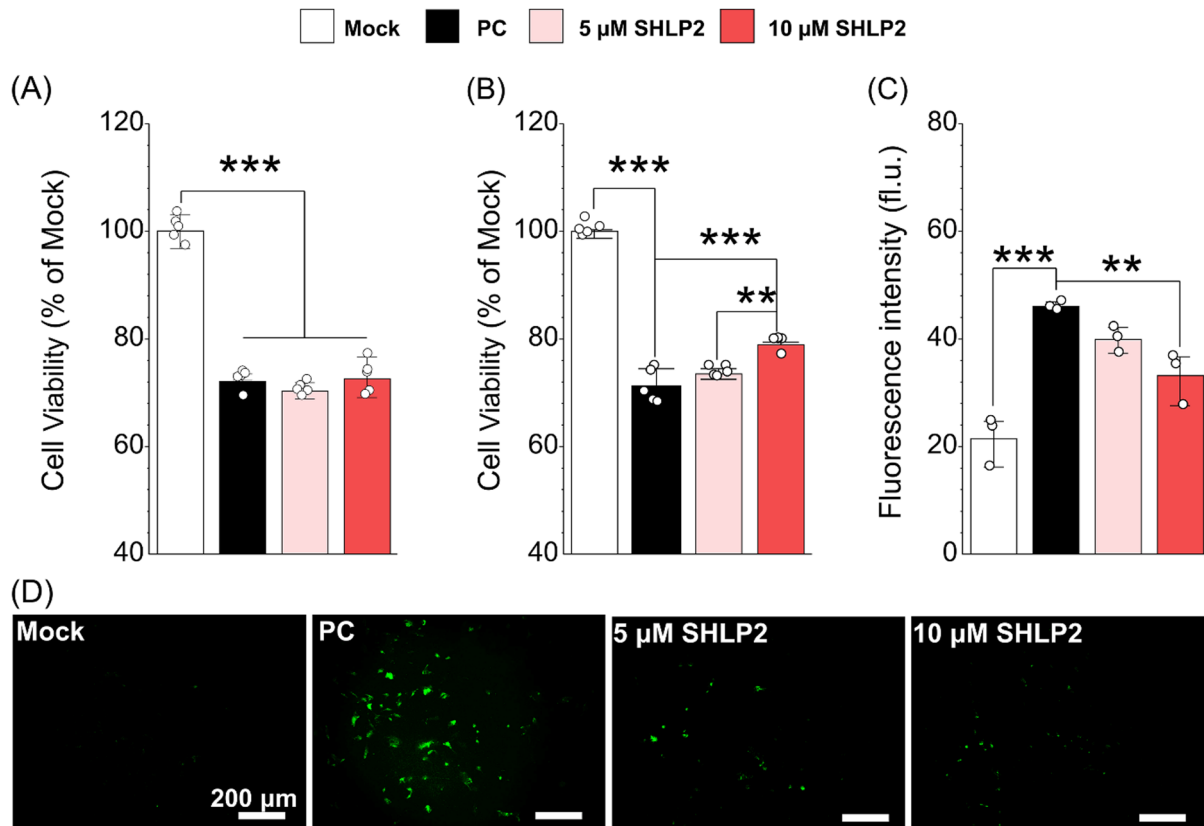


Fig. 2. Effects of SHLP2 treatment on cell viability and ROS detection in H_2O_2 -induced oxidative stress from MC3T3-E1 cells. Cell viability after SHLP2 treatment for (A) 1 day and (B) 3 days, performed by WST-1 assay following 24 h exposure to 600 μ M H_2O_2 ($n = 5$; ** $p < 0.01$; *** $p < 0.001$). (C) Quantitative fluorescence intensity of intracellular ROS after 24 h exposure to 600 μ M H_2O_2 ($n = 3$; ** $p < 0.01$, *** $p < 0.001$). (D) Representative fluorescence microscopy images showing ROS distribution in each group. Scale bar: 200 μ m. Data are presented as mean \pm SD. Mock, untreated pre-osteoblastic cells cultured by growth medium; PC, H_2O_2 -treated pre-osteoblastic cells cultured by growth medium. 5 μ M SHLP2, H_2O_2 -treated pre-osteoblastic cells cultured by growth medium containing 5 μ M SHLP2; 10 μ M SHLP2, H_2O_2 -treated pre-osteoblastic cells cultured by growth medium containing 10 μ M SHLP2. WST-1; water soluble tetrazolium-1; ROS, reactive oxygen species.

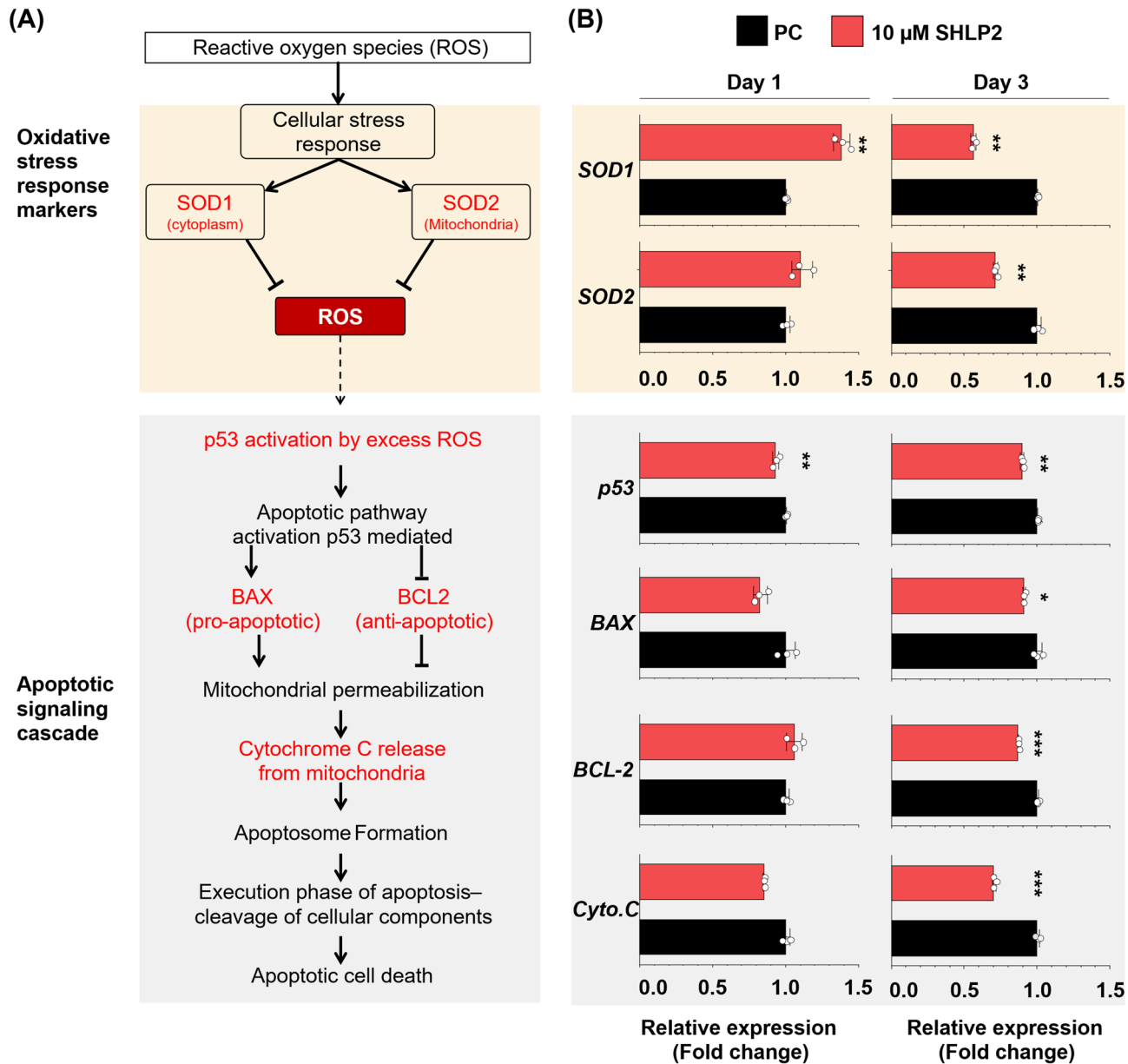


Fig. 3. Apoptosis expression assay of the oxidatively stressed MC3T3-E1 cells. **(A)** Schematic representation of oxidative stress response marker and the subsequent apoptotic signaling cascade. **(B)** Relative gene expression of apoptotic gene markers following treatment with 10 μ M SHLP2 in H_2O_2 -induced oxidative stress from MC3T3-E1 cells after 1 day and 3 days ($n=3$; * $p<0.05$; ** $p<0.01$; *** $p<0.001$). Data are presented as mean \pm SD. PC, H_2O_2 -treated pre-osteoblastic cells cultured by growth medium. 10 μ M SHLP2, H_2O_2 -treated pre-osteoblastic cells cultured by growth medium containing 10 μ M SHLP2.

significant upregulation of all markers, with multi-fold increases particularly in ALP, BSP, and OSX expression (Fig. 4B).

The 7-day ALP upregulation was corroborated by ALP staining (Fig. 5A). SHLP2 treatment significantly promoted osteoblastic activity, achieving 85.6% of the mock group's activity compared to 50% in the PC group. Furthermore, after 14 days of culture, the optical density (OD) levels indicative of ALP activity reached 95.6% of the mock group in the SHLP2-treated cells, compared to only 61.8% in the PC group (Fig. 5B).

These results indicate that 10 μ M SHLP2 substantially enhances osteogenic marker expression, demonstrating its potential to restore cellular activity in oxidatively stressed MC3T3-E1 cells.

SHLP2 enhanced mineralization in differentiating pre-osteoblastic cells

The late-stage osteogenic differentiation, assessed through the ARS biominerization assay, demonstrated marked osteoblastic activity in SHLP2-treated groups as early as day 14, achieving 94.9% of the mock group's response, compared to 68.5% in the PC group (Fig. 6A). By day 21, ARS staining intensity increased in both the

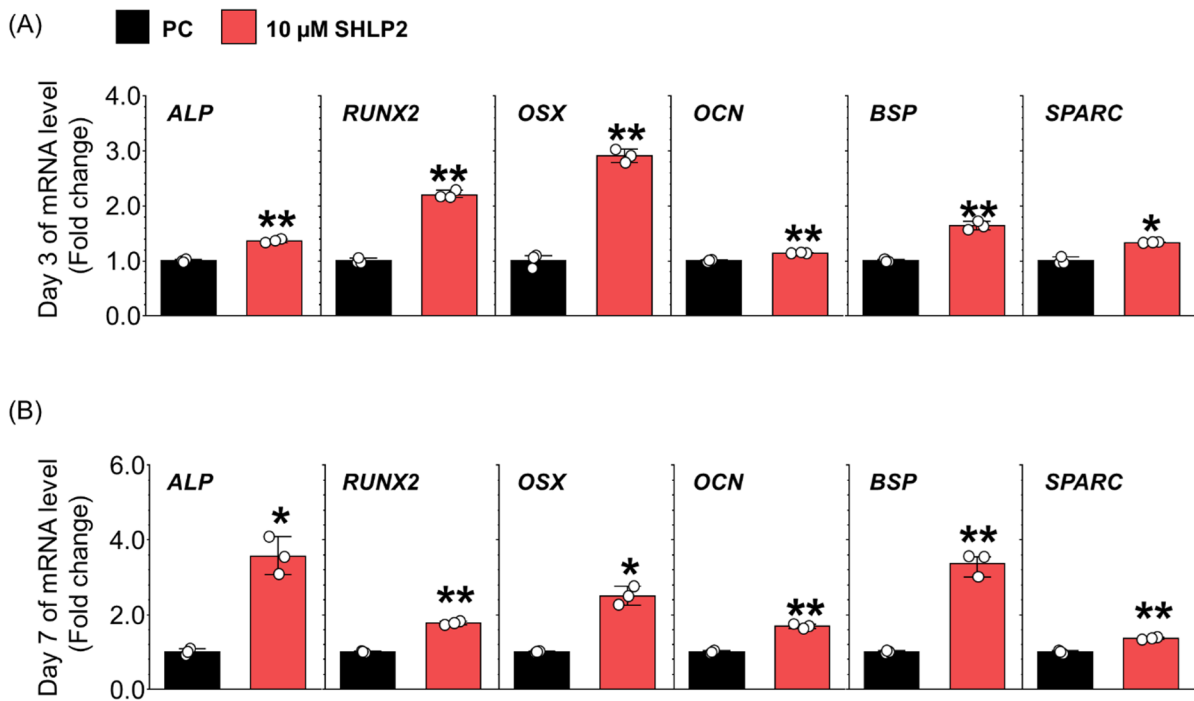


Fig. 4. Osteogenic expression assay of the oxidatively stressed MC3T3-E1. Relative gene expression of osteogenic gene markers following treatment with 10 μ M SHLP2 in H_2O_2 -induced oxidative stress from MC3T3-E1 cells after (A) 3 days and (B) 7 days ($n=3$; * $p<0.05$; ** $p<0.01$; *** $p<0.001$). Data are presented as mean \pm SD. PC, H_2O_2 -treated pre-osteoblastic cells cultured by osteogenic medium. 10 μ M SHLP2, H_2O_2 -treated pre-osteoblastic cells cultured by osteogenic medium containing 10 μ M SHLP2. ALP, alkaline phosphatase; RUNX2, runt-related transcription factor 2; OSX, osterix; OCN, osteocalcin; BSP, bone sialoprotein; SPARC, secreted protein acidic and cysteine rich.

PC and SHLP2-treated groups, indicating enhanced mineral deposition over time. However, relative to the mock group, the PC group exhibited significantly lower expression (72.1%) compared to the SHLP2-treated group, which maintained a high response at 94.9% (Fig. 6B).

Discussion

Mitochondrial-derived peptides, such as SHLP, exhibit cytoprotective properties that have been extensively studied in systemic degenerative disease models^{10,14–16}. Therefore, the present study investigates the cytoprotective effects of SHLP2 on sub-toxic oxidative stress, a key factor contributing to periodontal degeneration through cellular damage and premature senescence^{2,9,17}.

We modeled the murine pre-osteoblastic cell line under sub-toxic oxidative stress by treating cells with 600 μ M H_2O_2 to evaluate the mitigative effects of SHLP2 on osteoblast-lineage cell types. Our findings confirmed that exogenously administered SHLP2 did not adversely affect the viability of normal, stress-free cells. A recent study has proposed the existence of a feedback loop that exerts a counterbalancing effect to maintain the balance of mitochondrial peptides within the cell¹⁸. This observation aligns with our results, which demonstrated that increasing concentrations of SHLP2 did not compromise cellular viability. In addition, SHLP2 at 10 μ M effectively activates AMPK and ERK signaling through receptor-dependent mechanisms to regulate the cellular energy metabolism and oxidative balance in neuronal cells¹⁴. Our own dose-response screening experiments (5 and 10 μ M) in pre-osteoblastic cells confirmed that SHLP2 at the 10 μ M concentration showed higher cell viability and cytoprotective effects under oxidative stress.

Considering the improved viability of cells up to 10 μ M SHLP2 treatment, we investigated the effect on sub-toxic oxidative stress-induced MC3T3-E1¹⁹. Here, we confirmed a reversal of oxidative stress with the reduction in the ROS with SHLP2, specifically after treatment for 3 days²⁰. A similar protective role of humanin and its analog has been shown in earlier studies for smooth muscle cells, cortical neurons, macrophage, and hepatocytes^{13,16}. However, it is important to note that SHLP2 is structurally smaller than humanin¹¹, and in comparison, to the humanin analog, the effect of SHLP2 was significantly more pronounced at low concentrations (10 μ M)²⁰.

Accumulated sub-toxic oxidative stress is a contributor to inflammation dysregulation and periodontal disease pathogenesis²¹. Additionally, heightened ROS reaction triggers a cascade of intracellular response which subsequently trigger danger-associated molecular patterns (DAMPs)^{5,22}. Given the role of DAMPs in activating the inflammasome state, we investigated the SHLP2 treatment effect on the apoptotic pathway under the sub-toxic ROS levels²³. Our findings confirmed an effective early response on day 1, which peaked before day 3 showing a near reversal of the oxidative stress. Broadly, the ROS-associated apoptotic cascade is linked to mitochondrial DAMPs at three stages: the early reaction related to mitochondrial damage, the stage following

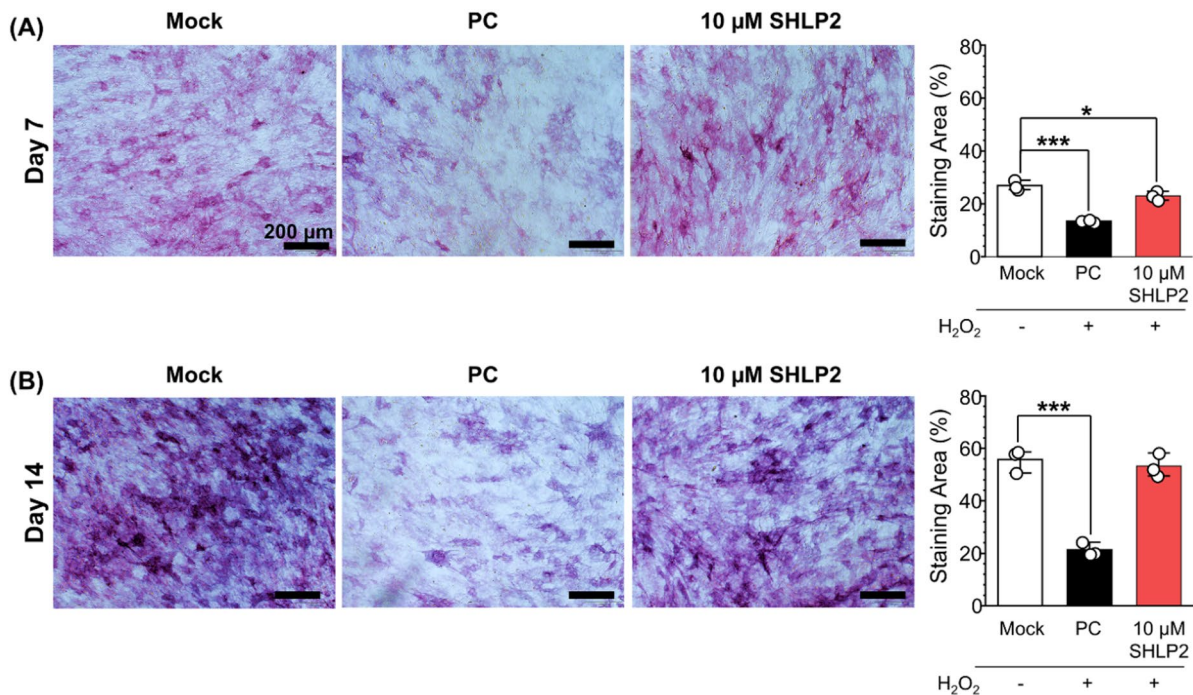


Fig. 5. Alkaline phosphatase staining assay of the oxidatively stressed MC3T3-E1 cells. Alkaline phosphatase staining in protein level following treatment with 10 μ M SHLP2 in H₂O₂-induced oxidative stress from MC3T3-E1 cells after (A) 7 days and (B) 14 days ($n=3$; * $p < 0.05$; *** $p < 0.001$). Scale bar: 200 μ m. Data are presented as mean \pm SD. Mock, untreated pre-osteoblastic cells cultured by osteogenic medium; PC, H₂O₂-treated pre-osteoblastic cells cultured by osteogenic medium; 10 μ M SHLP2, H₂O₂-treated pre-osteoblastic cells cultured by osteogenic medium containing 10 μ M SHLP2.

mitochondrial permeabilization, and the late stage near irreversible cellular damage^{24,25}. The findings in the present study confirm the retrograde signaling mechanism against ROS akin to other mitochondrial peptides²⁶.

The exogenously added SHLP2 demonstrated anti-apoptotic activity, accompanied by increased expression of antioxidant genes such as SOD1 and SOD2 and reduces ROS accumulation, similar to the protective effect reported for Humanin in reperfusion injury of intestinal cells²⁷. SHLP2 treatment also led to a reduction in BAX expression. Given the established role of the BAX-Humanin complex in apoptosis protection, these findings are consistent with SHLP2 influencing the osteoblast lineage via related pathways²⁸. The marked reduction in Cytochrome C expression, which is typically released from mitochondria following permeabilization, is also consistent with protection against mitochondrial-driven apoptosis²⁹. Nevertheless, protein-level validation is required; at transcriptional level, the observed changes indicate that SHLP2 is associated with reduced markers of mitochondrial stress and apoptosis under oxidative conditions.

In the context of natural bone healing, inflamming can lead to altered functional activity, characterized by increased expression of pro-apoptotic markers and suppression of osteogenic markers³⁰. The early anti-apoptotic effect of SHLP2 was demonstrated by its ability to promote favorable expression of both early and mature osteogenic differentiation markers. Notably, the significant improvement in ALP expression observed in day-14 markers, validated through PCR and staining, mirrored the levels seen in mock cells not exposed to oxidative stress. The functional expression of ALP is a vital step during the initial phase of the calcification mechanism driving the pyrophosphate formation³¹. Given the upregulation of ALP expression in oxidatively stressed pre-osteoblastic cells, it can be inferred that the SHLP2 treatment not only mitigated the apoptotic cascade but also promoted a restoration of physiological activity³⁰. With an expression of genes at distinct temporal sequence, MC3T3-E1 differentiates into mature osteoblasts and contributes to bone matrix mineralization. The SHLP2-treated group demonstrated upregulated expression of early-stage pro-osteogenic markers RUNX2 and OSX at day 3, along with a marked increase in BSP expression at day 7, further confirming the restoration of normalized osteogenic activity. These findings were similar to the rescue effect displayed by humanin on MC3T3-E1 cells with 400 μ M H₂O₂²⁰. However, in the present study sub-toxic oxidative effect was achieved at higher concentrations for a longer duration, indicating a strong efficacy with SHLP2 treatment. Subsequent observations of the biomineralization with ARS confirmed the above functional restoration of the oxidatively stressed pre-osteoblast cells with SHLP2 at 10 μ M concentration.

This study differs from previous investigations by demonstrating the osteogenic restorative capacity of SHLP2 in bone-forming cells exposed to chronic, sub-toxic oxidative stress conditions that mimic inflamming. While prior research on Humanin analogs has primarily addressed short-term cytoprotection, the present findings add to the evidence with SHLP2 supporting osteogenic recovery and mitochondrial redox homeostasis.

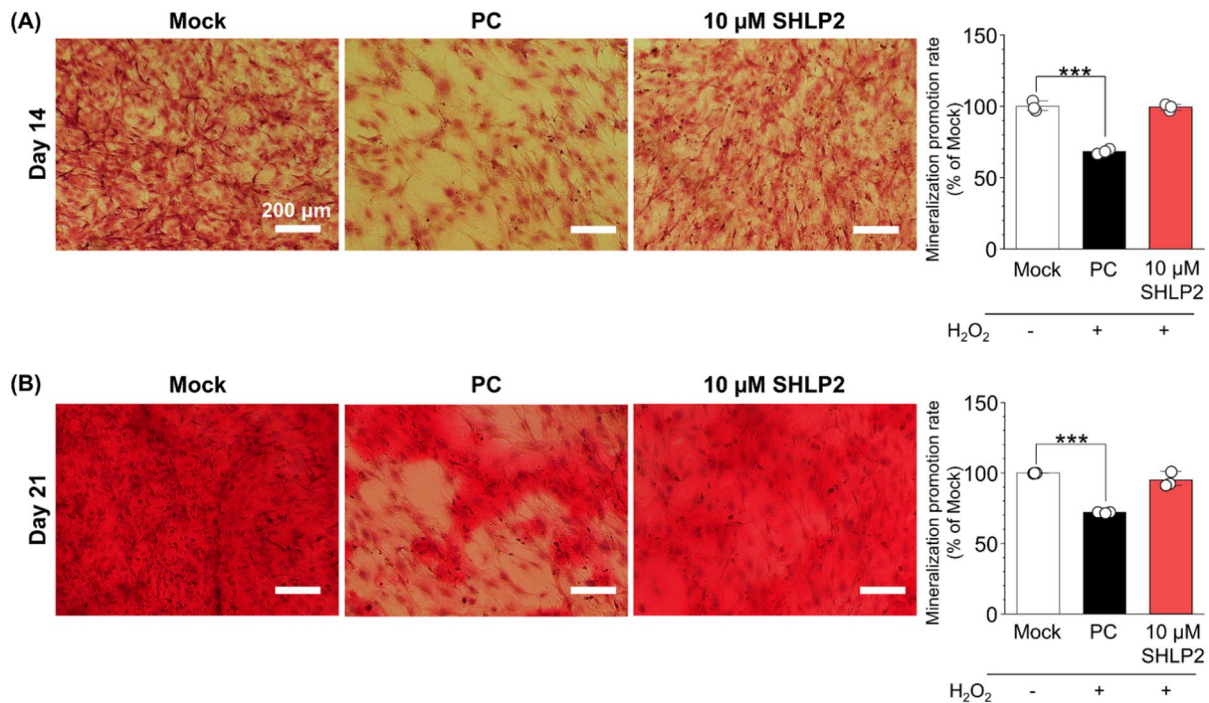


Fig. 6. Biominerization assay of the oxidatively stressed MC3T3-E1 cells. Alizarin Red S staining in protein level following treatment with 10 μ M SHLP2 in H_2O_2 -induced oxidative stress from MC3T3-E1 cells after (A) 14 days and (B) 21 days ($n=3$; * $p < 0.05$; *** $p < 0.001$). Scale bar: 200 μ m. Data are presented as mean \pm SD. Mock, untreated pre-osteoblastic cells cultured by osteogenic medium; PC, H_2O_2 -treated pre-osteoblastic cells cultured by osteogenic medium; 10 μ M SHLP2, H_2O_2 -treated pre-osteoblastic cells cultured by osteogenic medium containing 10 μ M SHLP2.

Here, SHLP2 treatment increased cellular metabolic activity, which we believe is synergistic with enhanced mitochondrial function and cell proliferation. All groups were seeded at equal densities and maintained comparable viability, indicating that the observed increases in ALP staining and mineralization represent functional recovery rather than proliferation-driven effects. Because SHLP2 was administered after oxidative stress induction, its role in this model appears mainly cytoprotective, restoring osteogenic function impaired by ROS rather than directly stimulating osteogenesis under basal conditions.

While this study confirmed transcriptional regulation of apoptotic and osteogenic markers, protein-level validation (e.g., BAX, BCL-2, cytochrome c) will be required to substantiate these findings. Future studies will also assess SHLP2 activity in the absence of oxidative stress to clarify its osteoinductive potential. This study has limitations, including the use of a single pre-osteoblastic cell line, whereas the periodontal microenvironment involves interactions among stem cells, fibroblasts, immune cells, and osteoclasts. Moreover, although this model captures chronic, low-grade oxidative stress, macrophage-driven inflammation and osteoclast coupling require further examination.

Given the significant role of SHLP2 identified here, future investigations are needed to explore its effects on other target cells within the periodontal microenvironment and to elucidate the network of interactions that drive tissue homeostasis. In addition, *in vivo* studies are warranted to confirm the therapeutic efficacy and biological safety of SHLP2 using a periodontitis model in future research. Taken together, targeted SHLP2 therapy may represent a promising strategy to mitigate periodontitis- and inflamming-associated alveolar bone loss by restoring osteoblastic function, thereby improving the tissue microenvironment and advancing periodontal regeneration.

Conclusion

In summary, treatment with 10 μ M SHLP2 effectively reversed oxidative stress in pre-osteoblastic cells, providing apoptosis protection while preserving osteogenic activity. These findings highlight the therapeutic potential of SHLP2 as an adjuvant strategy for improving the tissue microenvironment in periodontitis and inflamming. Nevertheless, this study was limited to a single pre-osteoblastic cell line, whereas the periodontal microenvironment is inherently complex, involving diverse cellular interactions, immune regulation, and osteoclast activity. Future investigations should therefore employ multicellular systems and *in vivo* models to further elucidate the broader role of SHLP2 in maintaining alveolar bone homeostasis and periodontal regeneration.

Methods

Cell culture

MC3T3-E1 osteoblast-like cells (mouse C57BL/6 calvaria, subclone 4; ATCC) were cultured in low-glucose Dulbecco modified eagle medium (DMEM, Cytiva, Marlborough, MA, United States) with 10% fetal bovine serum (FBS, Thermo Fisher Scientific, Waltham, MA, United States) and 1% penicillin-streptomycin (PS, Cytiva) at 37 °C in 5% CO₂, hereafter referred to as LG-DMEM. We used LG-DMEM, which contains a glucose concentration of approximately 5 mM, reflecting physiological levels. This condition was chosen to minimize the risk of experimental artifacts that may arise under supraphysiological glucose concentration, according to a previous study³². The growth medium was refreshed every three days, and subculturing was done at < 80% confluence using Trypsin/EDTA (Cytiva). Osteogenic medium included 50 µg/mL ascorbic acid and 10 mM β-glycerophosphate (Sigma-Aldrich, St. Louis, MO, United States) in the growth medium. The medium was replaced every 2 or 3 days.

Construction of the oxidative stress-induced cellular model

To construct the oxidative-induced cellular model as the sub-toxic threshold associated with cellular aging and inflammaging in a previous study³³, 1 × 10⁴ cells were plated in 96-well plates and treated with H₂O₂ (200, 400, 600, and 800 µM; 30% H₂O₂, Sigma Aldrich) for 24 h. After discarding the old medium, cytotoxicity was assessed using a WST-1 assay (EZ-Cytotox, DoGenBio, Republic of Korea). Fresh medium with 10% WST-1 was added, incubated for 1 h at 37 °C, and the optical density was measured at 450 nm (BioTek, Winooski, VT, USA). The concentration at which cell viability reached the 70% threshold was designated as the sub-toxic threshold dose.

Cytotoxicity of SHLP2 from pre-osteoblastic cells

Small humanin-like peptide 2 was synthesized by AnyGen (Gwangju, Republic of Korea) in a previous study¹⁴. 1 mg of SHLP2 was dissolved in 330 µL of sterile distilled water (Joongwae Pharmaceutical Co., Ltd., Seoul, Republic of Korea) to achieve a 1 mM concentration of SHLP2. To test SHLP2 cytotoxicity, each concentration of SHLP2 (5, 10, and 20 µM) was diluted from a 1 mM concentration of SHLP2 based on the growth medium. After that, MC3T3-E1 cells were treated with SHLP2 (5, 10, 20 µM) for 24 h, followed by the same WST-1 assay.

Mitochondrial activity assay

To assess cellular metabolic activity as an indicator of mitochondrial function, the WST-1 assay was performed. Cells were seeded at 2 × 10⁴ into the 24-well plate and incubated for 24 h at 37 °C in an atmosphere with 5% CO₂ and a humidified environment. After the initial 24 h attachment period, the culture medium was replaced with fresh growth medium containing 600 µM H₂O₂ and incubated for an additional 24 h to induce oxidative stress. Following H₂O₂ exposure, the cells were gently rinsed twice with Dulbecco's phosphate buffer saline without Ca²⁺ and Mg²⁺ (DPBS; Cytiva) to remove residual peroxide and then treated with fresh growth medium containing SHLP2 at the indicated concentrations for 1, 3, and 7 days. Untreated cells cultured in growth medium served as the mock, whereas H₂O₂-treated cells cultured in growth medium served as the positive control (PC).

At each time point, each well was treated with a 10% (v/v) WST-1 solution and subsequently incubated at 37 °C for 1 h. Then, the supernatant from each well was moved to 96-well plates. Optical density was measured at 450 nm by a microplate reader (Biotek, Winooski, VT, USA).

Reactive oxygen species detection assay

Intracellular ROS generation was assessed using the CellROX™ Green reagent (ThermoFisher Scientific). MC3T3-E1 cells were seeded at 5 × 10⁴ cells/well in 24-well plates and incubated for 24 h at 37 °C with 5% CO₂. After the initial 24 h attachment period, the culture medium was replaced with fresh growth medium containing 600 µM H₂O₂ and incubated for an additional 24 h to induce oxidative stress. Following H₂O₂ exposure, the cells were gently rinsed twice with Dulbecco's phosphate buffer saline without Ca²⁺ and Mg²⁺ (DPBS; Cytiva) to remove residual peroxide and then treated with fresh growth medium containing SHLP2 at the indicated concentrations for 24 h. Untreated cells cultured in growth medium served as the mock, whereas H₂O₂-treated cells cultured in growth medium served as the positive control (PC). For the fluorescence assay, 5 µM CellROX working solution was applied to cells for 30 min. After rinsing with DPBS and fixing with 3.7% paraformaldehyde, cells were examined under a fluorescence microscope (Olympus IX73; ×10 magnification). Fluorescence intensity was quantified using Zen software (version 3.4, Carl Zeiss).

Quantitative polymerase chain reaction

To examine apoptosis and osteogenic gene expression, quantitative polymerase chain reaction (qPCR) was conducted. MC3T3-E1 cells were seeded at 1 × 10⁵ cells/well in 12-well plates and incubated for 24 h at 37 °C with 5% CO₂. After the initial 24 h attachment period, the culture medium was replaced with fresh growth medium containing 600 µM H₂O₂ and incubated for an additional 24 h to induce oxidative stress. Following H₂O₂ exposure, the cells were gently rinsed twice with Dulbecco's phosphate buffer saline without Ca²⁺ and Mg²⁺ (DPBS; Cytiva) to remove residual peroxide. For the analysis of the apoptotic gene expression, the oxidative stress-induced cells were subsequently treated with growth medium containing SHLP2 at the indicated concentrations for 1 and 3 days. H₂O₂-treated cells cultured in growth medium served as the positive control (PC). For osteogenic gene expression, the oxidative stress-induced cells were cultured in osteogenic differentiation medium containing SHLP2 at the indicated concentration for 3 and 7 days. H₂O₂-treated cells cultured in osteogenic medium served as the positive control (PC). Total RNA was extracted using Qiazol (Qiagen, Hilden, Germany) per the manufacturer's protocol, and cDNA was synthesized using the PrimeScript™ RT kit (Takara Bio, Tokyo, Japan). qPCR was performed on a real-time PCR system with SYBR® Premix Ex Taq™

II (Takara Bio). Target gene primers (Bioneer, Daejeon, Republic of Korea) are detailed in Table S1. Relative expression levels were calculated via the $2^{-\Delta\Delta CT}$ method, with GAPDH as the internal control.

Alkaline phosphatase staining

To evaluate alkaline phosphatase (ALP) expression in oxidative stress-induced MC3T3-E1 cells, ALP staining was performed. MC3T3-E1 cells were seeded at 1×10^5 cells/well in 24-well plates. After the initial 24 h attachment period, the culture medium was replaced with fresh growth medium containing 600 μM H_2O_2 and incubated for an additional 24 h to induce oxidative stress. Following H_2O_2 exposure, the cells were gently rinsed twice with Dulbecco's phosphate buffer saline without Ca^{2+} and Mg^{2+} (DPBS; Cytiva) to remove residual peroxide and then treated with fresh growth medium containing SHLP2 at the indicated concentrations for 7 and 14 days. Untreated cells cultured in osteogenic medium served as the negative control (NC), whereas H_2O_2 -treated cells cultured in osteogenic medium served as the positive control (PC). After each time point, cells were fixed with 4% paraformaldehyde, washed, and stained with SIGMAFAST™ BCIP™/NBT reagent (Sigma Aldrich) at 25 °C for 1 h. Stained cells (purple) were observed under a light microscope at $\times 10$ magnification, and the ALP-stained area percentage was quantified using ImageJ³⁴.

Biomineralization assay

To evaluate biomineralization in oxidative stress-induced MC3T3-E1 cells, Alizarin Red S (ARS) staining was performed. MC3T3-E1 cells were seeded at 1×10^5 cells/well in 24-well plates. After the initial 24 h attachment period, the culture medium was replaced with fresh growth medium containing 600 μM H_2O_2 and incubated for an additional 24 h to induce oxidative stress. Following H_2O_2 exposure, the cells were gently rinsed twice with Dulbecco's phosphate buffer saline without Ca^{2+} and Mg^{2+} (DPBS; Cytiva) to remove residual peroxide and then treated with fresh growth medium containing SHLP2 at the indicated concentrations for 14 and 21 days. Untreated cells cultured in osteogenic medium served as the negative control (NC), whereas H_2O_2 -treated cells cultured in osteogenic medium served as the positive control (PC). After each time point, cells were fixed with 4% paraformaldehyde, washed, and stained with ARS solution (Sigma Aldrich). Mineralized nodules (red) were observed under a light microscope at $\times 10$ magnification. Quantification was performed by dissolving ARS in 10 mM sodium phosphate (pH 7.0) with 10% cetylpyridinium chloride, and optical density was measured at 562 nm using a microplate reader³⁵.

Statistical analysis

Statistical analyses were conducted using SPSS v26 (IBM, Armonk, NY, USA). All experiments were performed independently at least three times, with each condition tested in triplicate. Data presented as mean \pm standard deviation. Multiple-group comparisons were evaluated by one-way ANOVA with Tukey's post-hoc test, while differences between the two groups were assessed using a t-test. Significance was defined at $p < 0.05$.

Data availability

The data that support the findings of this study are available from the corresponding author upon reasonable request.

Received: 26 August 2025; Accepted: 25 November 2025

Published online: 29 November 2025

References

- Huang, X. et al. The roles of osteocytes in alveolar bone destruction in periodontitis. *J. Transl. Med.* **18**, <https://doi.org/10.1186/s12967-020-02664-7> (2020).
- Ebersole, J. L. et al. Aging, inflammation, immunity and periodontal disease. *Periodontol 2000* **72**, 54–75. <https://doi.org/10.1111/prd.12135> (2016).
- Hajishengallis, G. Too old to fight? Aging and its toll on innate immunity. *Mol. Oral Microbiol.* **25**, 25–37. <https://doi.org/10.1111/j.2041-1014.2009.00562.x> (2010).
- Franceschi, C. et al. Inflamm-aging. An evolutionary perspective on Immunosenescence. *Ann. N Y Acad. Sci.* **908**, 244–254. <https://doi.org/10.1111/j.1749-6632.2000.tb06651.x> (2000).
- Szczepanik, F. S. C. et al. Periodontitis is an inflammatory disease of oxidative stress: we should treat it that way. *Periodontol 2000* **84**, 45–68. <https://doi.org/10.1111/prd.12342> (2020).
- Albuquerque-Souza, E. et al. TLR9 mediates periodontal aging by fostering senescence and inflammaging. *J. Dent. Res.* **101**, 1628–1636. <https://doi.org/10.1177/00220345221110108> (2022).
- Patil, V. S., Patil, V. P., Gokhale, N., Acharya, A. & Kangokar, P. Chronic periodontitis in type 2 diabetes mellitus: oxidative stress as a common factor in periodontal tissue injury. *J. Clin. Diagn. Res.* **10**, BC12–16. <https://doi.org/10.7860/JCDR/2016/17350.7542> (2016).
- Duarte, P. M. et al. The expression of antioxidant enzymes in the gingivae of type 2 diabetics with chronic periodontitis. *Arch. Oral Biol.* **57**, 161–168. <https://doi.org/10.1016/j.anchoralbio.2011.08.007> (2012).
- Zhou, F., Wang, Z., Zhang, G., Wu, Y. & Xiong, Y. Immunosenescence and inflammaging: conspiracies against alveolar bone turnover. *Oral Dis.* **30**, 1806–1817. <https://doi.org/10.1111/odi.14642> (2024).
- Conte, M., Martucci, M., Chiariello, A., Franceschi, C. & Salvio, S. Mitochondria, Immunosenescence and inflammaging: a role for mitokines? *Semin Immunopathol.* **42**, 607–617. <https://doi.org/10.1007/s00281-020-00813-0> (2020).
- Cobb, L. J. et al. Naturally occurring mitochondrial-derived peptides are age-dependent regulators of apoptosis, insulin sensitivity, and inflammatory markers. *Aging (Albany NY)* **8**, 796–809. <https://doi.org/10.18632/aging.100943> (2016).
- Nashine, S. & Kenney, M. C. Effects of mitochondrial-derived peptides (MDPs) on mitochondrial and cellular health in AMD. *Cells* **9**, 1102 (2020).
- Choi, I. A., Umemoto, A., Mizuno, M. & Park-Min, K. H. Bone metabolism – An underappreciated player. *Npj Metab. Health Dis.* **2**, <https://doi.org/10.1038/s44324-024-00010-9> (2024).
- Kim, S. K. et al. Mitochondria-derived peptide SHLP2 regulates energy homeostasis through the activation of hypothalamic neurons. *Nat. Commun.* **14**, 4321. <https://doi.org/10.1038/s41598-023-40082-7> (2023).

15. Thummasorn, S. et al. Humanin directly protects cardiac mitochondria against dysfunction initiated by oxidative stress by decreasing complex I activity. *Mitochondrion* **38**, 31–40. <https://doi.org/10.1016/j.mito.2017.08.001> (2018).
16. Thamarai Kannan, H., Issac, P. K., Dey, N., Guru, A. & Arockiaraj, J. A. Review on mitochondrial derived peptide humanin and small humanin-like peptides and their therapeutic strategies. *Int. J. Pept. Res. Ther.* **29**. <https://doi.org/10.1007/s10989-023-1055-8-7> (2023).
17. Muller, F., Srinivasan, M., Krause, K. H. & Schimmel, M. Periodontitis and peri-implantitis in elderly people experiencing institutional and hospital confinement. *Periodontol 2000* **90**, 138–145. <https://doi.org/10.1111/prd.12454> (2022).
18. Nashine, S., Cohen, P., Nesburn, A. B., Kuppermann, B. D. & Kenney, M. C. Characterizing the protective effects of SHLP2, a mitochondrial-derived peptide, in macular degeneration. *Sci. Rep.* **8**, 15175. <https://doi.org/10.1038/s41598-018-33290-5> (2018).
19. Quarles, L. D., Yohay, D. A., Lever, L. W., Caton, R. & Wenstrup, R. J. Distinct proliferative and differentiated stages of murine MC3T3-E1 cells in culture: an *in vitro* model of osteoblast development. *J. Bone Min. Res.* **7**, 683–692. <https://doi.org/10.1002/jbm.r.5650070613> (1992).
20. Zhu, X. et al. HNGF6A inhibits oxidative stress-induced MC3T3-E1 cell apoptosis and osteoblast phenotype Inhibition by targeting Circ_0001843/miR-214 pathway. *Calcif Tissue Int.* **106**, 518–532. <https://doi.org/10.1007/s00223-020-00660-z> (2020).
21. Rattanaprakskul, K. et al. Molecular signatures of senescence in periodontitis: clinical insights. *J. Dent. Res.* **103**, 800–808. <https://doi.org/10.1177/00220345241255325> (2024).
22. Chapple, I. L. & Matthews, J. B. The role of reactive oxygen and antioxidant species in periodontal tissue destruction. *Periodontol 2000* **43**, 160–232. <https://doi.org/10.1111/j.1600-0757.2006.00178.x> (2007).
23. Gonzalez, O. A., Kirakodu, S. S. & Ebersole, J. L. DAMPs and alarmin gene expression patterns in aging healthy and diseased mucosal tissues. *Front. Oral Health.* **4**, 1320083. <https://doi.org/10.3389/froh.2023.1320083> (2023).
24. Koenig, A. & Buskiewicz-Koenig, I. A. Redox activation of mitochondrial damps and the metabolic consequences for development of autoimmunity. *Antioxid. Redox Signal.* **36**, 441–461. <https://doi.org/10.1089/ars.2021.0073> (2022).
25. Murao, A., Aziz, M., Wang, H., Brenner, M. & Wang, P. Release mechanisms of major damps. *Apoptosis* **26**, 152–162. <https://doi.org/10.1007/s10495-021-01663-3> (2021).
26. Lee, C., Yen, K. & Cohen, P. Humanin: a harbinger of mitochondrial-derived peptides? *Trends Endocrinol. Metab.* **24**, 222–228. <https://doi.org/10.1016/j.tem.2013.01.005> (2013).
27. Abozaid, E. R., Abdel-Kareem, R. H. & Habib, M. A. A novel beneficial role of humanin on intestinal apoptosis and dysmotility in a rat model of ischemia reperfusion injury. *Pflugers Arch.* **475**, 655–666. <https://doi.org/10.1007/s00424-023-02804-0> (2023).
28. Jumaa, H. et al. Deficiency of the adaptor SLP-65 in pre-B-cell acute lymphoblastic leukaemia. *Nature* **423**, 452–456. <https://doi.org/10.1038/nature01608> (2003).
29. Wolter, K. G. et al. Movement of Bax from the cytosol to mitochondria during apoptosis. *J. Cell. Biol.* **139**, 1281–1292. <https://doi.org/10.1083/jcb.139.5.1281> (1997).
30. Kushioka, J. et al. Bone regeneration in inflammation with aging and cell-based Immunomodulatory therapy. *Inflamm. Regen.* **43**, 29. <https://doi.org/10.1186/s41232-023-00279-1> (2023).
31. Vimalraj, S. Alkaline phosphatase: Structure, expression and its function in bone mineralization. *Gene* **754**, 144855. <https://doi.org/10.1016/j.gene.2020.144855> (2020).
32. Busch, M., White, N., Shum, L. & Eliseev, R. A. Active mitochondria support osteogenic differentiation by stimulating β -catenin acetylation. *J. Biol. Chem.* **293**, 16019–16027 (2018).
33. Han, D. et al. Cytoprotective effect of chlorogenic acid against hydrogen peroxide-induced oxidative stress in MC3T3-E1 cells through PI3K/Akt-mediated Nrf2/HO-1 signaling pathway. *Oncotarget* **8**, 14680 (2017).
34. Collins, T. J. ImageJ for microscopy. *Biotechniques* **43**, 25–30. <https://doi.org/10.2144/000112517> (2007).
35. Ryu, J. H. et al. Synergistic effect of porous hydroxyapatite scaffolds combined with bioactive glass/poly(lactic-co-glycolic acid) composite fibers promotes osteogenic activity and bioactivity. *ACS Omega* **4**, 2302–2310. <https://doi.org/10.1021/acsomega.8b02898> (2019).

Author contributions

J.H.R. Data curation, Formal analysis, Methodology, Writing – original draft, Funding acquisition. U.M. Data curation, Formal analysis, Visualization, Writing – original draft, Investigation, Writing - Review & Editing. J.H.K and D.J.Y: Investigation, Methodology. K.J.L: Supervision and Resource, Y.H.C: Supervision, Resource, D.M.S: Supervision and Resource, S.H.C: Conceptualization, Methodology, Supervision, Writing - Review & Editing, Project administration, Funding acquisition. K.W.K: Conceptualization, Supervision, Writing - Review & Editing, Project administration, Funding acquisition. All authors reviewed the manuscript. J.H.R and U.M. have co-first authorship based on equal contributions.

Funding

This work was supported by the National Research Foundation of Korea (NRF) grant funded by the Korea government (MSIT) (No. RS-2023-00217709). This work was supported by the National Research Foundation of Korea (NRF) grant funded by the Korea government (MSIT) (No. RS-2024-00346807, No. RS-2024-00338986, No. RS-2024-00357334, and No. RS-2025-18362970). This research was supported by the Regional Innovation System & Education(RISE) program through the Gangwon RISE Center, funded by the Ministry of Education(MOE) and the Gangwon State(G.S.), Republic of Korea.(2025-RISE-10-101)(P0028969, Regional Anchor-company-Academia Partnership Innovation Development. This study was supported by a Yonsei-Dentium research grant of Yonsei University College of Dentistry (6-2023-0218).

Declarations

Competing interests

The authors declare no competing interests.

Additional information

Supplementary Information The online version contains supplementary material available at <https://doi.org/10.1038/s41598-025-30415-5>.

Correspondence and requests for materials should be addressed to S.-H.C. or K.W.K.

Reprints and permissions information is available at www.nature.com/reprints.

Publisher's note Springer Nature remains neutral with regard to jurisdictional claims in published maps and institutional affiliations.

Open Access This article is licensed under a Creative Commons Attribution-NonCommercial-NoDerivatives 4.0 International License, which permits any non-commercial use, sharing, distribution and reproduction in any medium or format, as long as you give appropriate credit to the original author(s) and the source, provide a link to the Creative Commons licence, and indicate if you modified the licensed material. You do not have permission under this licence to share adapted material derived from this article or parts of it. The images or other third party material in this article are included in the article's Creative Commons licence, unless indicated otherwise in a credit line to the material. If material is not included in the article's Creative Commons licence and your intended use is not permitted by statutory regulation or exceeds the permitted use, you will need to obtain permission directly from the copyright holder. To view a copy of this licence, visit <http://creativecommons.org/licenses/by-nc-nd/4.0/>.

© The Author(s) 2025